Proceedings of Global Power and Propulsion Society
ISSN-Nr: 2504-4400
GPPS Hong Kong 2023
October 17-19, 2023
www.gpps.global

GPPS-TC-2023-0126

Influence of Blowing Ratio on Double-Wall Cooling Characteristics under the Condition of High-temperature Flue Gas

Baichuan Yi
Key Laboratory of Advanced Energy and Power, Institute of Engineering Thermophysics, Chinese Academy of Sciences; University of Chinese Academy of Sciences
yibaichuan@iet.cn
Beijing, China

Yan Xiong
Key Laboratory of Advanced Energy and Power, Institute of Engineering Thermophysics, Chinese Academy of Sciences; University of Chinese Academy of Sciences
*corresponding author: xiongyan@iet.cn
Beijing, China

Zhigang Liu
Key Laboratory of Advanced Energy and Power, Institute of Engineering Thermophysics, Chinese Academy of Sciences; University of Chinese Academy of Sciences
liuzhigang@iet.cn
Beijing, China

Yan Liu
Key Laboratory of Advanced Energy and Power, Institute of Engineering Thermophysics, Chinese Academy of Sciences; University of Chinese Academy of Sciences
liuyan@iet.cn
Beijing, China

Xiaopo Wei
Jiangsu Zhongke Research Center for Clean Energy and Power
weixiaopo@jscep.ac.cn
Lianyungang, China

ABSTRACT

Double-wall cooling structure has been widely studied due to its excellent cooling performance. Most of the previous studies on the cooling characteristics of double-wall have been carried out in the non-reacting conditions without considering the influence of high-temperature flue gas radiation. In this paper, an experiment was carried out to assess the effect of blowing ratio M on cooling characteristics of effusion/impingement cooling at reacting flow conditions. The experiment was performed at atmospheric pressure with adiabatic flame temperature of the flue gas reaching 1800 K. The flue gas temperature was measured by S type thermocouples. The temperature distribution on the wall was measured by an infrared camera and N type thermocouples. The results show that the laterally averaged cooling effectiveness of effusion/impingement cooling system increases with the increase of M. After M>3, the effect on cooling effectiveness is no longer obvious. The laterally averaged cooling effectiveness gradually increases along the flow direction, while its growth rate slows down. Meanwhile, the cooling effectiveness remains basically unchanged after X/D>50.

INTRODUCTION

Gas turbine is widely used in aviation, power generation, and maritime applications. With the pursuit of high-performance gas turbines, the exit temperature of the combustion chamber has increased in recent years, vastly beyond the material's tolerance limit (Hada et al., 2012; Naik, 2017). Meanwhile, NOx and other pollutant emission control regulations are getting increasingly strict. More air is required for combustion to meet low-emissions regulations, and the air available for combustion tube cooling is decreasing (Lefebvre et al., 2010). Furthermore, as the working temperature of the combustion chamber rises, so does the expected lifetime of the hot-end components. For these reasons, creating effective cooling structures has become critical.

Due to its superior performance, double-wall cooling is gaining popularity. The cooling process of the double wall is as follows： an array of cooling air jets first passes through the perforated baffle and impact the cold side of the effusion plate; then, the coolant flow into the effusion hole to forms forced convection heat transfer within the hole; and finally flows out and create a uniform and continuous protective film on the hot side wall of the effusion plate. The following are some benefits of the double-wall cooling technique: (1) The average heat transfer coefficient of the double-wall structure on the cold side of the effusion plate is 6–10 times higher than the ones achieved with effusion alone (Cho et al., 2001), taking full advantage of the high heat transfer coefficient of impingement cooling to cool local hot regions. (2) The

suction of the attached surface layer at the entrance of the evacuated hole enhances the heat transfer, increasing the target surface heat transfer coefficient by 45–55% in comparison to impingement cooling only(Cho et al.,1996).

Numerous investigations have been conducted on the double-wall cooling structure, including the effects of double-wall aerodynamic parameters, geometrical structural alterations, and so on. Rogers et al. (Rogers et al., 2017) investigated the effect of blowing ratio on effusion/impingement cooling efficiency under cross-flow conditions and found that the cooling efficiency increased along the streamwise direction, and the disturbance increased due to the formation of a horseshoe vortex at the position leaving the film orifice, resulting in an increase in the heat transfer coefficient. Legrani et al. (Ligrani et al., 2018) discovered that when the effusion coolant is supplied by an array of impingement cooling jets, the cooling effectiveness is higher than with a cross-flow channel supply system. Huelsmann et al. (Huelsmann et al., 2021) studied the influence of the position of the impingement hole relative to the effusion hole on the convective heat transfer performance within the effusion hole. The results showed a strong sensitivity to the circumferential and radial placement of the impingement jet. The degree of heat transfer enhancement caused by different positions ranges from 10% to 30%. In contrast, the jet-to-effusion distance has little effect. Bai et al. (Bai et al., 2023) experimentally investigated the effects of gap distance, impingement hole diameter, and effusion hole arrangement on cooling efficiency. They found that the increase in gap distance weakened the strength of the impingement jet and thus reduced the overall cooling performance. The smaller the impingement hole diameter, the weaker the cooling layer, resulting in a lower overall cooling performance at the same blowing ratio. Murray et al. (Murray et al., 2017; Murray et al., 2018) evaluated the impact of circular pin-fin diameter and spacing on aerothermal and thermomechanical performance using numerical and experimental methods. The findings revealed that lowering the pedestal diameter and spacing improved heat transfer while increasing thermal stress. Numerical simulation is utilized to obtain the flow field distribution inside the double-walled construction.

Most previous experimental studies were conducted in the non-reactive state, and the majority of them were consistent with the actual combustion chamber operating conditions by controlling the similarity parameters (Reynolds number, Nusselt number, Biot number, etc.); the main flow was rectified to obtain a uniform incoming temperature; and the boundary conditions of the experiments were more precise. Because the mainstream air temperature of such trials is lower, and the influence of radiation at lower temperatures is not apparent, more desired cooling results are frequently obtained (Behrendt et al., 2008). In the operational environment of a real combustion engine, however, the temperature and flow fields in the combustion chamber fluctuate with the flame morphology, affecting the temperature distribution on the wall (Ji et al., 2018; Ahmed et al., 2022). Furthermore, because the incoming flow temperature is higher in the reactive state than in the non-reactive state, the effect of radiation is enhanced. Thus, an experimental investigation of the characteristics of double-wall cooling in the reactive state is required.

The influence of the blowing ratio on double wall cooling in the reaction state is investigated in this work, and the temperature distribution on the hot side of the wall is recorded using an infrared camera and thermcouples, with its cooling efficiency and temperature uniformity trends evaluated.

METHODOLOGY

Experimental configurations

The schematic of the experimental system is shown in Figure 1. Experiment system is mainly composed of a 24-nozzles array combustor, fuel supply system, air supply system, double-wall experimental section, and temperature measurement system. Methane is used in the experiment, which is supplied from a high-pressure cylinder and controlled by a mass flow meter. The air is divided into the main flow and the coolant. The primary flow air is mixed with methane in the combustor， depicted in the study by Liu (Liu et al., 2022). The coolant flow into the test region, which is composed of three same double wall cooling plates and an infrared window. Details of the test plate are introduced in Table.1. Multiple thermocouples are laid on the film plate to measure the wall temperature（Figure 2). A type S thermocouple is installed at the leading edge of the test section to measure the gas temperature.

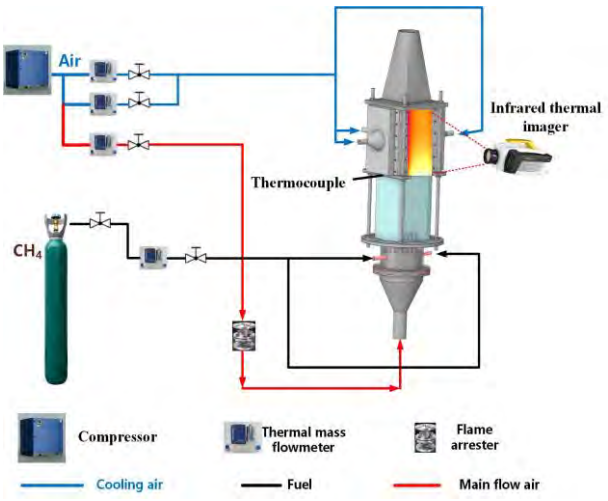

Figure 1 Sketch of experimental system

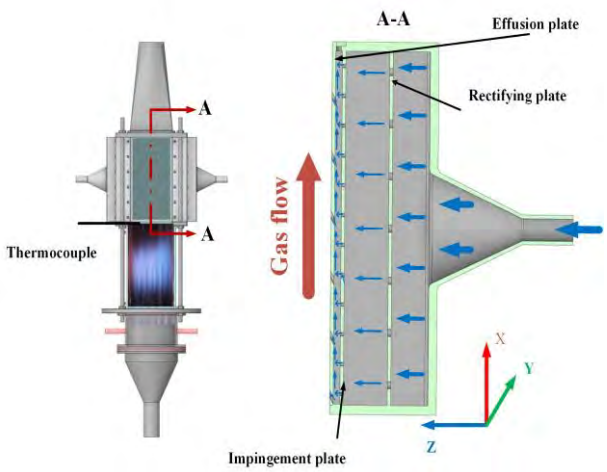

(a)

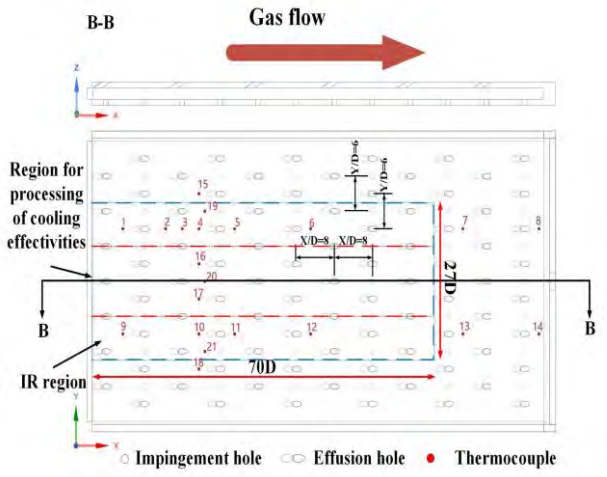

(b)

Figure 2 Details of the Test section: (a)Details of the double-wall structure;(b) Test plate

Table 1 details of the double-wall structure

Geometric parameters	value
Film/Impingement hole diameter D(mm)	2
Film hole Inclination（deg）	30
Film/Impingement plate thickness (mm)	2
Streamwise spacing of film/impingement holes Pholes,X/D	8
Lateral spacing of film/impingement holes Pholes,Y/D	6
Jet-to-target plate spacing Z/D	1

IR measurement and calibration

Infrared thermography is adopted to conduct surface temperature steady-state measurements on the hot side of test plates by the Telops FAST M200 infrared camera equipped with a pre-calibrated filter. The temperature measurement range is 206-1708 ℃, and the accuracy is 1%. The spatial resolutions are 640*512. A critical step that must be taken seriously is calibration, which determines the credibility of the temperature data. In this experiment, IR camera and calibration thermocouples at specifically selected locations record the temperature simultaneously once a steady state is reached. By comparing the temperature measured by IR camera and thermocouples, a calibration curve is fitted for the entire estimated temperature range. Figure 3 shows the calibration curve for IR measurements, and it can be found that the curve fitting is linear and has a relative error not exceeding $\pm 5\%$.A thin layer of high emissivity black paint is applied to the test plate to make it diffusely reflected, so it can be regarded as a gray body to handle the emissivity.

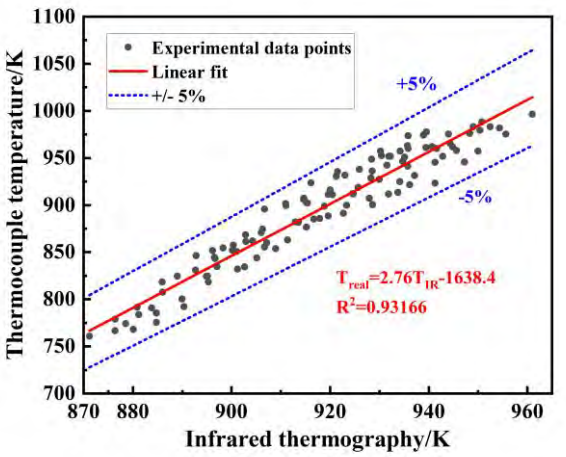

Figure 3 Calibration of IR measurements

Surface temperature on the hot side is used to estimate the cooling effectiveness, which characterizes the synthetic cooling ability of the Impingement/effusion cooling. The cooling effectiveness is defined as:

$$\eta = \frac{T_g - T_w}{T_g - T_c} \tag{1}$$

T_w is the test plate wall temperature after correction, and T_c is the cooling air temperature before entering plenums. T_g is the flue gas temperature measured by type S thermocouple. The flue gas temperature measured by the thermocouple is corrected using the Kaskan W E method (Kaskan et al., 1957). The corrected flue gas temperature is defined as Eq. (2).

$$T_g = T_b + \frac{1.25\varepsilon\sigma T_b^4 d_b^{0.75}}{\lambda}\left(\frac{\mu}{\rho V}\right)^{0.25} \tag{2}$$

Where T_g and T_b are the corrected flue gas temperature and measured temperature, respectively. ε is the emissivity of thermocouple. σ is Stefan-Boltzmann constant. D is the Characteristic length of thermocouple. λ , μ , ρ , V are the thermal conductivity , dynamic Viscosity , density and velocity of flue gas at measured temperature, respectively.

Operation conditions

Pure methane was used in the experiment. The primary airflow and the coolant are supplied at 289 K and atmospheric pressure. The flame temperature, T_f, is the calculated equilibrium temperature by Chemkin software based on air temperature and equivalence ratio, Φ. In this experiment, the flame temperature is set at 1800 K. The bulk velocity, u, is calculated from the combustor mass flow rate, flame temperature, flue gas density and cross-sectional area. The bulk speed of the hot gas flow can be set to about 8m/s. Blowing ratio is an important parameter for Impingement/effusion cooling systems defined by:

$$M = \frac{\rho_c V_c}{\rho_\infty V_\infty} = \frac{m_c}{m_\infty}\frac{A_\infty}{A_c} \tag{3}$$

Where ρ_c and V_c are the density and velocity of the jet, respectively; ρ_∞ and V_∞ are the density and velocity of the main flow, respectively. It can also be expressed as the ratio of the mass flow rate of cool air and hot air per unit area. In the experiment the value of A_∞/A_c and m_∞ is constant，so we can change the coolant mass flow rate to get a certain blowing ratio. The operating conditions in the test section are shown in Table.2.

Table2 Operating conditions in the test section

Variables	Values
Equilibrium temperature(K)	1800
Measured gas temperature(K)	1425
Corrected gas temperature(K)	1577
Coolant temperature(K)	289
Pressure(atm)	1
Blowing ratio	1-3.5
Bulk velocity(m/s)	8

RESULTS AND DISCUSSION

Wall temperature distribution

Figure 4 depicts the distribution of wall temperature at various blowing ratios. The picture demonstrates that for blowing ratios ranging from 1 to 3.5, the wall temperature does not exceed 1150 K. The highest temperatures are concentrated in the X/D<1.5 region, where there is no cooling air covering. The temperature on the Y>0 side is higher than that on the Y<0 side, which is caused by the asymmetrical temperature distribution of the Upstream flue gas in the reaction state. Figure 5 shows the distribution of cooling efficiency on the test plate corresponding to Figure 4. As shown in the picture, the cooling efficiency increases gradually along the flow direction. The region of low cooling efficiency is concentrated upstream of the test plate; when the blowing ratio increases, the area of this region shrinks significantly.

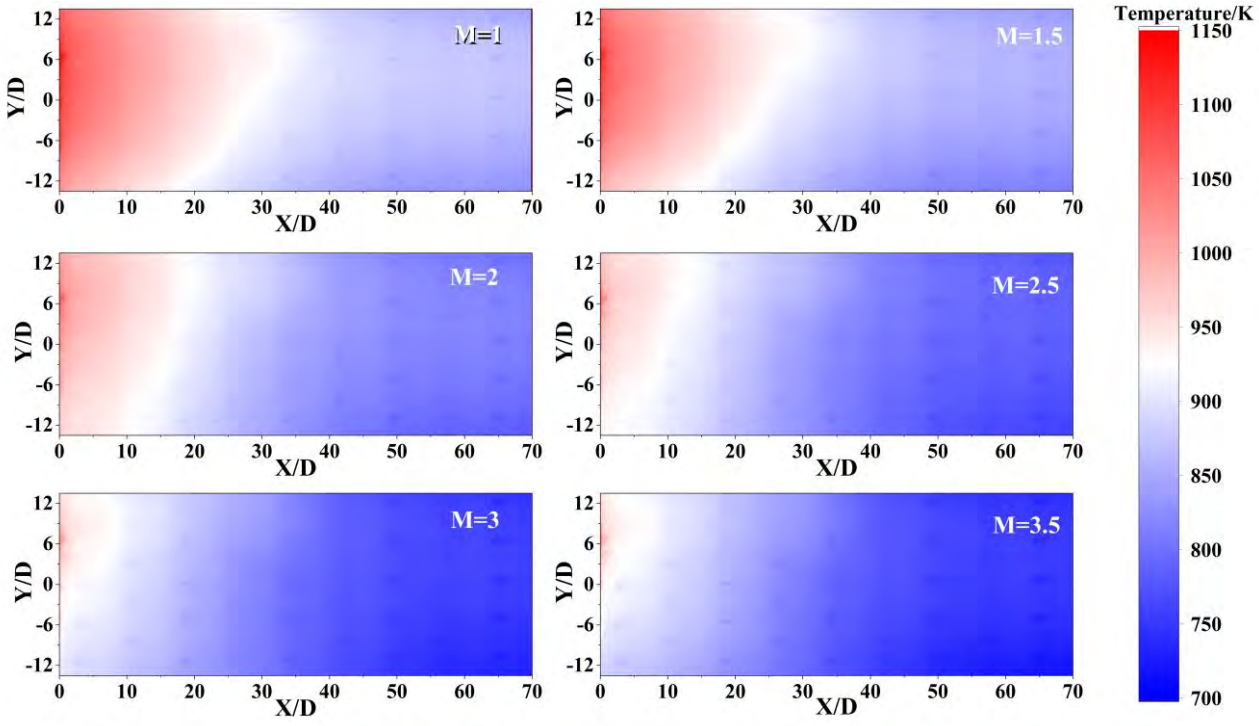

Figure 4 Wall temperature distribution

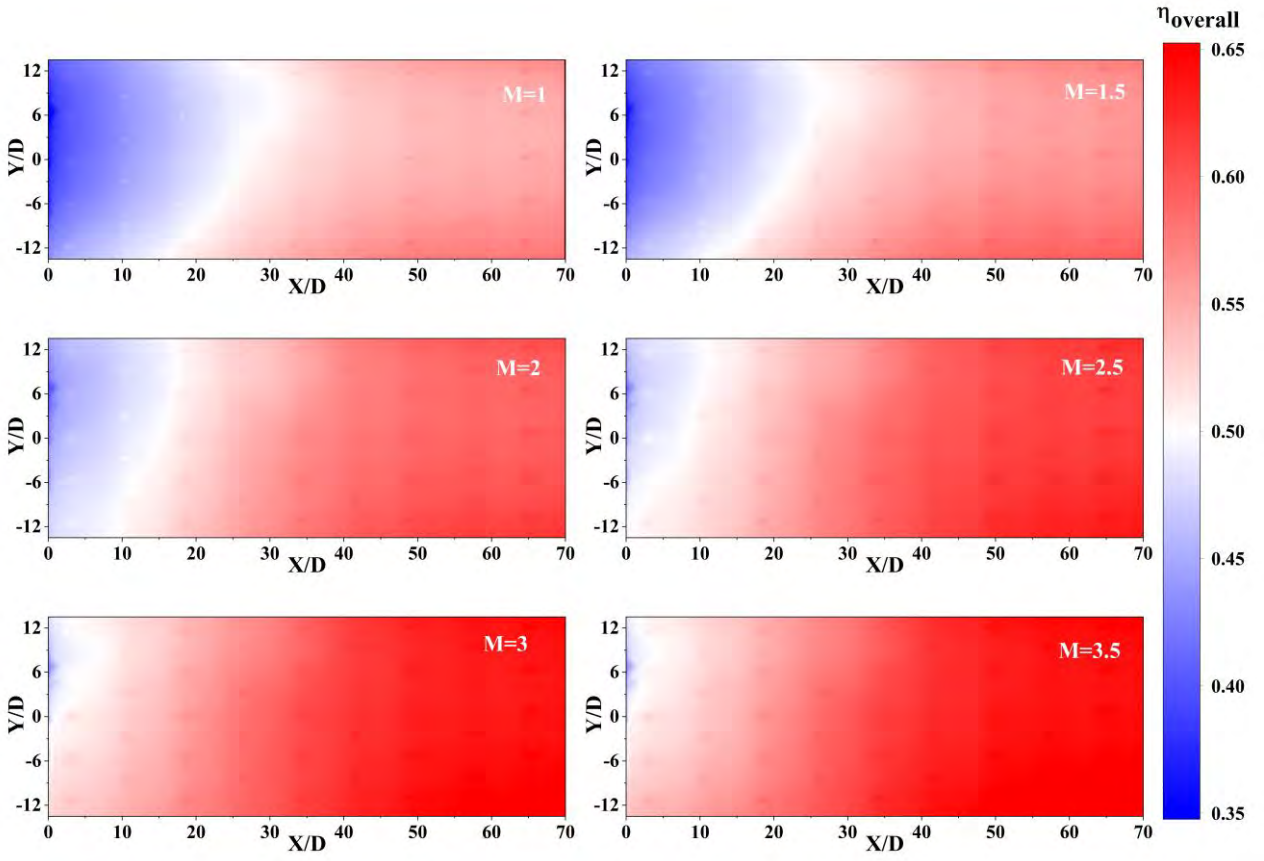

Figure 5 Overall cooling effectiveness distribution

The standard deviation of temperature at measuring sites in the cooling unit was computed by Eq. (4) to evaluate the homogeneity of temperature dispersion on the wall surface of the effusion plate.

$$\delta = \sqrt{\frac{\sum_{1}^{j}(\mathrm{T}_{i,j} - \bar{T}_i)}{j-1}} \qquad (4)$$

Where i is the flow direction pixel point, j is the lateral direction pixel point, and $\bar{T}_i$ is the laterally averaged temperature for each flow location i. We can utilize this equation to assess the inhomogeneity of the temperature distribution in the lateral direction at each flow direction position i, as well as its variation along the flow direction. To minimize the influence of thermocouples installed on the wall on the flow field, the temperature inhomogeneity is analyzed using a range of -6 < Y/D < 6.

Figure 6 shows the variation of temperature inhomogeneity along the flow direction for various blowing ratios, together with the placements of the effusion holes. Temperature inhomogeneity decreases along the streamwise direction in general. The inhomogeneity increases slightly between the third and fifth rows of effusion holes, most likely due to the effect of the thermocouples inserted in this location on the flow field. Meanwhile, the inhomogeneity of the wall temperature increases near the effusion holes. At the leading edge of the plate (X/D=0), the higher the blowing ratio, the larger the inhomogeneity of the wall temperature. The inhomogeneity of wall temperature reduces rapidly along the airflow direction before the first row of holes and then slows down afterward. The inhomogeneity decreases faster as the blowing ratio increases.

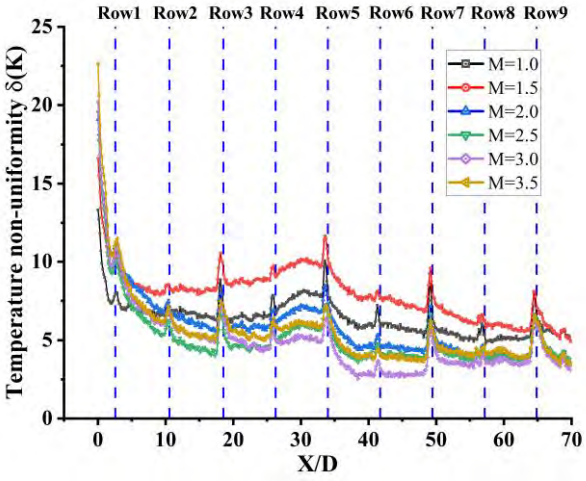

Figure 6 Variation of the temperature non-uniformity along the flow direction

Laterally averaged cooling effectiveness

Figure 7 illustrates the lateral-averaged cooling effectiveness varies along the flow direction for varied blowing ratios. It is evident that the laterally averaged cooling efficiency sharply increases along the direction of flow in the region before the first rows ($0 < X/D < 1.5$), and that this rise is correlated with an increase in the blowing ratio. This is because increasing the blowing ratio improves convective heat transfer inside the hole and on the cold side wall of the film plate. The lateral average cooling efficiency grows apparently along the flow direction in the $1.5 < X/D < 50$, while the trend of improvement gradually slows down. After X/D>50, the film thickness in this region is already significantly larger than the length scale of the mixing process in the shear layer between hot gas and coolant, and the inflow of cooling air cools the near-wall component of the film, leading the wall temperature decrease further(Behrendt et al., 2008). The cooling efficiency is approaching a steady state, and a fully developed stable film exists.

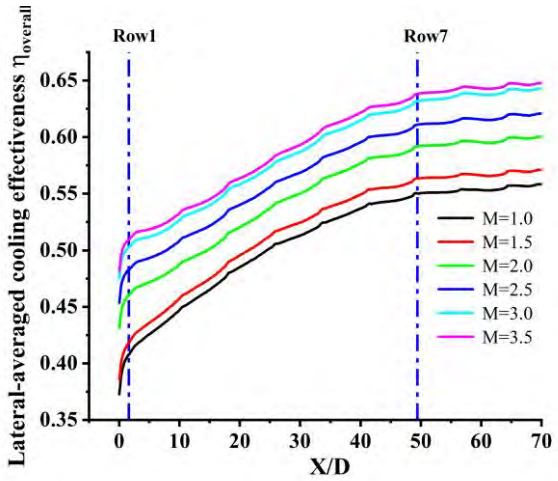

Figure 7 Lateral-averaged cooling effectiveness along the flow direction

Area-averaged overall cooling effectiveness

Figure 8 depicts the area-average cooling efficiency at various blowing ratios, with the area-average cooling efficiency increasing most when the blowing ratio is increased from 1.5 to 2. After M> 2, when the blowing ratio grows, the area averaged cooling efficiency increases, the growth rate slows down. The average cooling efficiency of the surface rose by 1.02% when the blowing ratio was increased from 3 to 3.5, at this time, increasing the blowing ratio for the ddouble-wallcooling efficiency is essentially no aid, but increased the consumption of cold air.

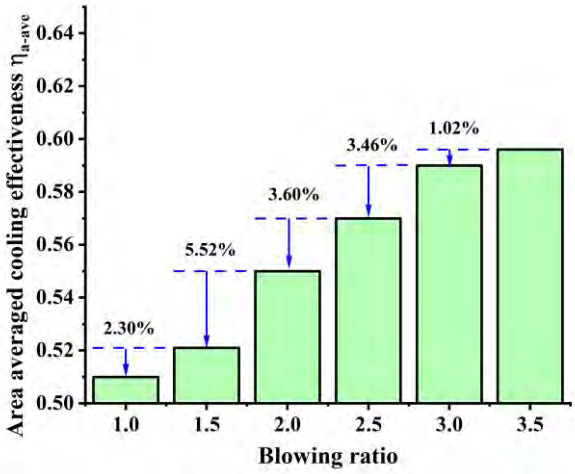

Figure 8 Effect of blowing ratio on area averaged cooling effectiveness

CONCLUSIONS

In order to provide data support for the subsequent design of double-wall cooling, the experimental study of the double-wall cooling characteristics at reactive conditions is presented in this work. The following findings were drawn after researching the effects of the blowing ratio on the double wall cooling characteristics.

1. As the blowing ratio rises, the temperature of the wall becomes more unequal in the region prior to the first row of holes. After the first rows of effusion holes, the wall temperature gradually becomes uniform along the flow direction, and as the blowing ratio rises, the non-uniformity of the wall temperature reduces more quickly.

2. The cooling efficiency rises along the airflow direction, while the growth rate decreases, and the cooling efficiency essentially remains unchanged after X/D>50.

3. The cooling effectiveness of the double wall increases with the increase of the blowing ratio; however, this effect is less significant in blowing ratios higher than 3.

CKNOWLEDGMENTS

The authors gratefully acknowledge the support provided by National Science and Technology Major Project of China (No.2019-III-0020-0064).

NOMENCLATURE

η	cooling effectiveness
$\eta_{a\text{-}ave}$	area-averaged overall cooling effectiveness
X/D	streamwise position
δ	temperature inhomogeneity

i	streamwise pixel point	
j	lateral pixel point	
T_c	cooling air temperature	[K]
T_w	wall temperature	[K]
T_b	measured gas flue temperature	[K]
T_g	corrected gas flue temperature	[K]
M	blowing ratio	
m_∞	mass flow rate of gas	[kg/s]
m_c	mass flow rate of coolant	[kg/s]
ρ	density	[kg/m^3]
ρ_∞	density of flue gas	[kg/m^3]
ρ_c	density of coolant	[kg/m^3]
A_∞	area of the cross-sectional	[m^2]
A_c	area of effusion holes	[m^2]
V_c	jet velocity	[m/s]
V_∞	flue gas velocity	[m/s]
d_b	characteristic length of the thermocouple	[m]
λ	thermal conductivity	[W/(m·K)]
Φ	global equivalence ratio	[-]
μ	dynamic viscosity of flue gas	[Pa·s]
ε	emissivity of thermocouple	[-]
σ	radiation constant of black body	[W/(m^2·K^4)]

REFERENCES

Ahmed, S., Ramakrishnan, K. R. and Ekkad, S. V. (2022). Overall Cooling Effectiveness of Effusion Cooled Can Combustor Liner Under Reacting and Non-Reacting Conditions. *Journal of Thermal Science and Engineering Applications, 14*(2), pp. 021009. https://doi.org/10.1115/1.4051371

Bai, N., Fan, W., Zhu, J., Miao, H., Yang, X., Zhao, Y., Zhao, W. and Zhang, R. (2023). Experimental investigations into the effusion plate wall temperature of impingement/effusion cooling systems for gas turbine combustors. *Aerospace Science and Technology, 132*, pp. 108052. https://doi.org/10.1016/j.ast.2022.108052

Behrendt, T. and Hassa, C. (2008). A test rig for investigations of gas turbine combustor cooling concepts under realistic operating conditions. *Proceedings of the Institution of Mechanical Engineers, Part G: Journal of Aerospace Engineering, 222*(2), pp. 169-177. https://doi.org/10.1243/09544100JAERO288

Cho, H. H., and Goldstein, R. J. (1996). Effect of hole arrangements on impingement/effusion cooling. In *KSME/JSME Thermal and Fluid Engineering Conference*, pp. 71-76.

Cho, H. H. and Rhee, D. H. (2001). Local Heat/Mass Transfer Measurement on the Effusion Plate in Impingement/Effusion Cooling Systems. *Journal of Turbomachinery, 123*(3), pp. 601-608. https://doi.org/10.1115/1.1344904

Hada, S., Tsukagoshi, K., Masada, J. and Ito, E. (2012). Test Results of the World's First 1,600C J-series Gas Turbine. *Mitsubishi Heavy Industries Technical Review*, *49*(1), pp. 18-23.

Huelsmann, N. C. and Thole, K. A. (2021). Effects of Jet Impingement on Convective Heat Transfer in Effusion Holes. *Journal of Turbomachinery, 143*(6), pp. 061011. https://doi.org/10.1115/1.4050335

Ji, Y., Ge, B., Chi, Z. and Zang, S. (2018). Overall cooling effectiveness of effusion cooled annular combustor liner at reacting flow conditions. *Applied Thermal Engineering, 130*, pp. 877-888. https://doi.org/10.1016/j.applthermaleng.2017.11.074

Kaskan, W. E. (1957). The dependence of flame temperature on mass burning velocity. *Symposium (International) on Combustion, 6*(1), pp. 134-143. https://doi.org/10.1016/S0082-0784(57)80021-6

Lefebvre, A. H., and Ballal, D. R. (2010). *Gas turbine combustion: alternative fuels and emissions*. 3rd ed. CRC press.

Ligrani, P., Ren, Z., Liberatore, F., Patel, R., Srinivasan, R. and Ho, Y.-H. (2018). Double Wall Cooling of a Full-Coverage Effusion Plate, Including Internal Impingement Array Cooling. *Journal of Engineering for Gas Turbines and Power, 140*(5), pp. 051901. https://doi.org/10.1115/1.4038248

Liu, Z., Xiong, Y., Zhang, Z., Ren, L., Liu, Y. and Lu, Y. (2022). Investigation of a novel combustion stabilization mechanism and combustion characteristics of a multi-nozzle array model combustor. *Fuel, 327*, pp. 125138. https://doi.org/10.1016/j.fuel.2022.125138

Murray, A. V., Ireland, P. T. and Rawlinson, A. J. (2017). An Integrated Conjugate Computational Approach for Evaluating the Aerothermal and Thermomechanical Performance of Double-Wall Effusion Cooled Systems. in *ASME Turbo Expo 2017: Turbomachinery Technical Conference and Exposition*: American Society of Mechanical Engineers. pp. V05BT22A015. https://doi:10.1115/GT2017-64711

Murray, A. V., Ireland, P. T. and Romero, E. (2018). Development of a Steady-State Experimental Facility for the Analysis of Double-Wall Effusion Cooling Geometries. https://doi.org/10.1115/GT2018-75924

Naik, S. (2017). Basic Aspects of Gas Turbine Heat Transfer. *Heat Exchangers - Design, Experiment and Simulation*, pp. 111-142 https://doi.org/10.5772/67323

Rogers, N., Ren, Z., Buzzard, W., Sweeney, B., Tinker, N., Ligrani, P., Hollingsworth, K., Liberatore, F., Patel, R., Ho, S. and Moon, H.-K. (2017). Effects of Double Wall Cooling Configuration and Conditions on Performance of Full-Coverage Effusion Cooling. *Journal of Turbomachinery,*

139(5), pp. 051009. https://doi.org/10.1115/1.4035277